

# Extraction, Characterization, and Application of Seaweed Nanoparticles on Cotton Fabrics

J. Mercy Sheeba, S. Thambidurai

Department of Industrial Chemistry, Alagappa University, Karaikudi 630003, India

Received 12 December 2008; accepted 5 February 2009

DOI 10.1002/app.30207

Published online 27 April 2009 in Wiley InterScience (www.interscience.wiley.com).

**ABSTRACT:** The seaweed *Turbinaria conoides* was collected from the east seashore of the south India. The dried seaweeds were converted into fine powder, mixed with acetone, and their antibacterial substance was extracted. The extracted substance was characterized by the use of Fourier transform infrared spectroscopy and ultraviolet-visible spectroscopy for functional group identification. The presence of bromine, amine, and phenolic groups was confirmed. Nanosized particles were confirmed by trans-

mission electron microscopy studies. The extract was applied on the enzyme scoured and dyed cotton fabric for bioantibacterial finish. The antibacterial activity of extract on the finished fabric was confirmed by the test results. © 2009 Wiley Periodicals, Inc. *J Appl Polym Sci* 113: 2287–2292, 2009

**Key words:** seaweed; antibacterial; FTIR; TEM; nanoparticle

## INTRODUCTION

Textiles, especially those made of natural fibers, are an excellent medium for the growth of microorganisms when the basic requirements such as nutrients, moisture, oxygen, and appropriate temperature are present. The large surface area and ability to retain moisture of textiles also assist the growth of microorganisms on the fabric. Therefore, there is a great demand for antimicrobial finishes of textiles to control the growth of microorganisms, such as bacteria, fungi, or mildew and prevent the textile from deterioration of strength and quality, staining, odors, and health concerns caused by microorganisms.<sup>1</sup>

At present, more synthetic antibacterial nanoparticles are developed and applied on textiles because of their novel properties and low material consumption of nanoparticles.<sup>2</sup> Nano-zinc oxide (ZnO) acts as an excellent antibacterial agent on cotton fabric, with slight reduction on tensile strength.<sup>3,4</sup> Scanning electron microscopy (SEM) characterization and biocidal tests of bleached cotton fabrics coated with an average size of 40 nm nanoparticles showed that nano ZnO antibacterial cotton fabric was relatively sensitive to acid artificial sweat while durable in saline or alkaline solution.<sup>5</sup> In case of nano-ZnO-coated fabric, because of its nanosize and uniform distribution, friction was significantly lower than the bulk-ZnO-coated fabric.<sup>6</sup> Nano silver-treated garments control

bacterial growth even after fifty washes, thereby providing lasting cleanliness and freshness.<sup>7</sup>

To replace the synthetic chemicals from antibacterial finishing, research is ongoing to find bioactive agents from natural products. Recent research shows that seaweed can be used for isolation of antibacterial agents. Along with antibacterial activity, seaweed also is used for nutritional purposes<sup>8</sup> and to remove metal ions from wastewater.<sup>9</sup>

Indian brown seaweeds, viz., *Sargassum marginatum*, *Padina tetrastomatica*, and *Turbinaria conoides*, were tested for antibacterial activity. Among the seaweeds, total methanolic extract of *T. conoides* had significantly greater phenol content ( $P < 0.05$ ) compared with the other two species.<sup>10,11</sup> Quantitative analysis of the total phenolic content of the seaweeds indicated that high phenolic contents, which correlated to their respective antioxidant and antimicrobial activity.<sup>12</sup> Sheu et al.<sup>13</sup> isolated nine new cytotoxic oxygenated fucosterols compounds from the marine brown alga *T. conoides* and found only six exhibit cytotoxicity against various cancer cell lines. Tuney et al.<sup>14</sup> found that antibacterial activity is in correlation with the degree of contamination in seawater and there is a significant seasonal difference in antibacterial activity of seaweeds.<sup>15</sup>

For an efficient strategy of investigation, organic solvents are used to extract the possible lipid-soluble active principles from macroalgae.<sup>16</sup> Previous studies have shown that methanol extraction can yield higher antimicrobial activity than hexane and ethyl acetate,<sup>17</sup> although in others, chloroform was more effective than methanol and benzene.<sup>13</sup> Kumar and Rengasamy<sup>15</sup> reported that chloroform extracts and

Correspondence to: S. Thambidurai (sthambi01@yahoo.co.in).

chloroform: methanol (2 : 1 v/v) extracts of red macro algae exhibited the maximum antibacterial activity, whereas the extracts of benzene, methanol, and ethanol showed only traces of activity. The structure of extract was determined by researchers using different techniques.<sup>18,19</sup>

In our earlier study,<sup>20</sup> diethyl ether solvent was used for extraction of bioactive substance from the seaweed. In the present investigation, an attempt was made to extract bioactive substance using acetone as a solvent and characterized by ultraviolet (UV) and Fourier transform infrared (FTIR) spectroscopy. Furthermore, the extracted bioactive substance was subjected to transmission electron microscopy (TEM) analysis for nanoparticles and applied on cotton fabric for antibacterial property.

## EXPERIMENTAL

### Extraction of antibacterial substance

Fresh weeds of *T. conoides* were collected at Gulf of Mannar in the east seashore of south India and washed with seawater followed by thorough washing with freshwater.<sup>20</sup> These were then dried under shade for 48 h until the moisture was completely removed; they then were grounded well in a mortar. The powdered seaweed sample was mixed with acetone at material to liquor ratio of 1 : 25. The mixture was stored in a dark place for 24 h at room temperature.<sup>10</sup> The supernatant liquid were transferred separately into sterile screw cap test tube and stored at room temperature in the dark.

### Bioscouring of cotton fabric

Bioscouring of acid desized cotton fabric (ends/inch: 140; picks/inch 80, count: 40 s, weight/sq. cm 0.015 g) was conducted in a programmable HTHP beaker-dyeing machine using pectinase enzyme (2 g/L) with liquor ratio of 1 : 10. The pH was maintained at 4.5 with the use of citric acid/sodium acetate buffer. The temperature was slowly increased to 50°C and maintained for 1 h. Then, the fabric was taken out, washed thoroughly with water, and the residual enzymes were deactivated by increasing the temperature to 80°C for 10 min. They are then cooled, washed thoroughly, and finally rinsed with distilled water and air dried.

### Dyeing

Cotton fabrics were dyed with direct dye according to the conventional exhaustion method in a laboratory dyeing apparatus. The dye bath was applied at dye concentration 2% shade, liquor ratio of 1 : 30 and temperature of 90°C. The dyed samples were

washed with a soap solution (2 g/L) at 50°C for 30 min, washed with tap water, and finally with distilled water and dried at ambient conditions.

### Antibacterial finish

The finishing solution was prepared by mixing the acetone extract (20 mL/L) and starch solution (30 g/L) with liquor ratio 1 : 20. The bioscouring and dyed cotton fabric was entered in to the solution and kept for 20 min. Then the fabric taken out and padded in the padding mangle and air dried at room temperature.

## Characterization and testing

### Spectral studies

The extract containing the antibacterial substance was examined for functional group identification with UV-visible spectroscopy (2401 PC model; Shimadzu, Kyoto, Japan) in the wavelength range of 200–800 nm and FTIR spectroscopy (PerkinElmer RX1 model; PerkinElmer, Waltham, MA) in the spectral range of 4000 to 400  $\text{cm}^{-1}$ .

### Transmission electron microscopy

The supernatant liquid of 20 mL was centrifuged at 4000 rpm and 20°C for 20 min in the Kubota 6800 Refrigerated Ultra Centrifuge machine (Kubota Corp., Tokyo, Japan). Then the sample was taken out, the clear acetone was removed, and the residue of extract transferred on the glass plate to get complete dry. The fine particles were collected and then examined in TEM (JEOL1200EX 120 kV TEM; JEOL, Tokyo, Japan).

### Antibacterial test

The antibacterial tests were performed as per the standard test procedure ATCC 6538 according to SN 195920. Treated cotton fabric was tested against the Gram-negative bacterium *Escherichia coli*. Fresh inoculants for antibacterial assessment were prepared on nutrient agar at 37°C for 48 h. All tests on specimens in liquid culture were conducted in nutrient broth. To prepare an agar plate, solid culture was prepared by mixing 2 g of agar-agar, 0.5 g of peptone, and 0.3 g of beef extract in 100 mL of distilled water. One hundred microliters of microbial culture was uniformly distributed on the plate. Treated cotton fabric of 5 mm width was placed on the plate. The plate was placed in an incubator for 24 h at 37°C. The zone of inhibition was then measured and recorded.

## RESULTS AND DISCUSSION

### UV-visible spectroscopy

This technique is very useful to measure the number of conjugated double bonds and also used to measure the aromatic conjugation within the various molecules. The electronic excitation occurs in the region of 200–800 nm. UV spectra of seaweed extract solution and its transition and absorption maxima are shown in the Figure 1. In the UV spectrum the near UV region between 230 and 270 nm shows a broad absorption band. This B bands (Benzenoid bands) are characteristic of aromatic molecules. A band at  $\lambda_{\max}$  281 nm is observed at longer wavelength than the more intense  $\pi-\pi^*$  transition. It occurs when the chromophoric group is attached to an aromatic ring.

The absorption band at 281 nm shows the presence of carbonyl group due to this carbonyl group  $\pi-\pi^*$  transition takes place. The  $\pi-\pi^*$  (R bands) occur in the 350–370 nm region shows the presence  $\alpha,\beta$ -unsaturated ketone.

The band at 471 nm shows the presence of 11 internal double bonds. Because of the lycopene it produces the absorption band at 476 nm. It has the 11 external double bonds. The presence of absorption band near 662 nm shows the nitroso group.<sup>19</sup>

### FTIR spectra

The FTIR spectrum of the seaweed extract was taken at the region 4000–400  $\text{cm}^{-1}$  and divided in to three regions. Figure 2 shows the spectrum of the 1400–600  $\text{cm}^{-1}$  region. The peak appearing between 644 and 531  $\text{cm}^{-1}$  is attributed to the O–C–N bending

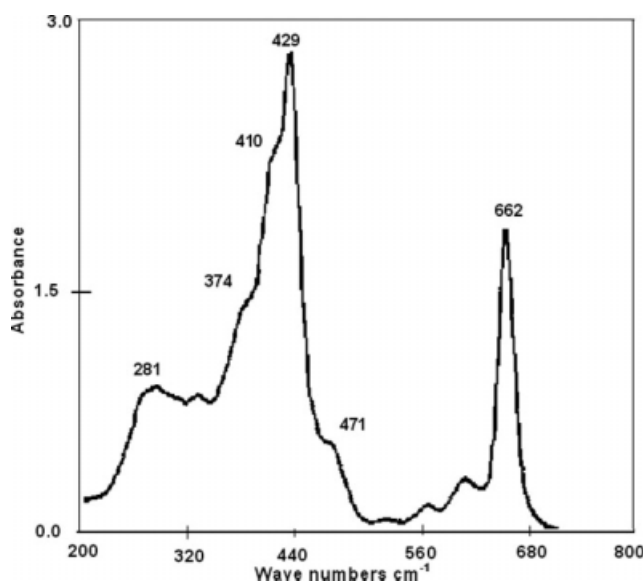


Figure 1 UV spectra of seaweed extract.

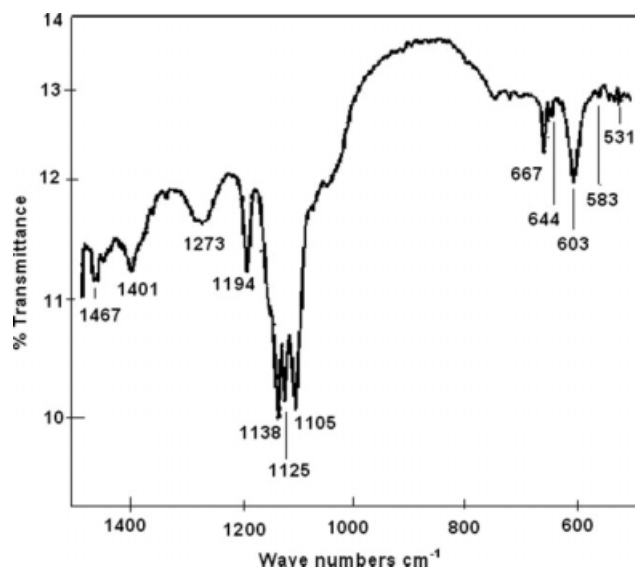


Figure 2 FTIR spectra of seaweed extract (1400–600  $\text{cm}^{-1}$ ).

vibration of the amide group (amide IV & VI bands). The strong band around 1105  $\text{cm}^{-1}$  received due to the C–O stretching. It shows the presence of secondary alcohols. The symmetry band at 1125 and 1138  $\text{cm}^{-1}$  attributed to alcoholic C–O–C stretching frequency.

A strong absorbance at 1273  $\text{cm}^{-1}$  is caused by the S=O asymmetric stretching vibration of sulphate groups.<sup>21</sup> A band at 583  $\text{cm}^{-1}$ , is due to O–S–O asymmetric deformation of sulphate groups.<sup>22</sup> The sulfate group is considered a highly selective anti-herpetic compound, with antiviral effectiveness, particularly against the TK<sub>1</sub> strains of HSV-1.<sup>23</sup>

The sharp moderate intensity band at 1138  $\text{cm}^{-1}$  is caused by asymmetric C–N–C stretching vibration with respect of the amide group. The sharp band at 1194  $\text{cm}^{-1}$  also shows the presence of C–CO–C stretching vibration. Aliphatic primary and secondary amines with primary carbons exhibit medium intensity band at 1138  $\text{cm}^{-1}$  due to asymmetric C–C–N and C–N–C stretching vibration respectively. The medium intensity band at 1401  $\text{cm}^{-1}$  is caused by the C–N stretching vibration of amide III band. The absorption band at 1467  $\text{cm}^{-1}$  obtained by the methylene scissoring and methyl asymmetric bending modes. This shows the molecules contain both methyl and methylene group.

Figure 3 shows the spectrum of the 2000–1600  $\text{cm}^{-1}$  region. A medium intensity band at 1620  $\text{cm}^{-1}$  caused by  $\text{NH}_2$  bending vibration appears in secondary amine salts. The symmetric and asymmetric NH bending vibration in primary amine salts occur at 1620  $\text{cm}^{-1}$  and 1555 and 1507  $\text{cm}^{-1}$  assigned to bands I, II, and III of the amide function of proteins.<sup>24</sup>

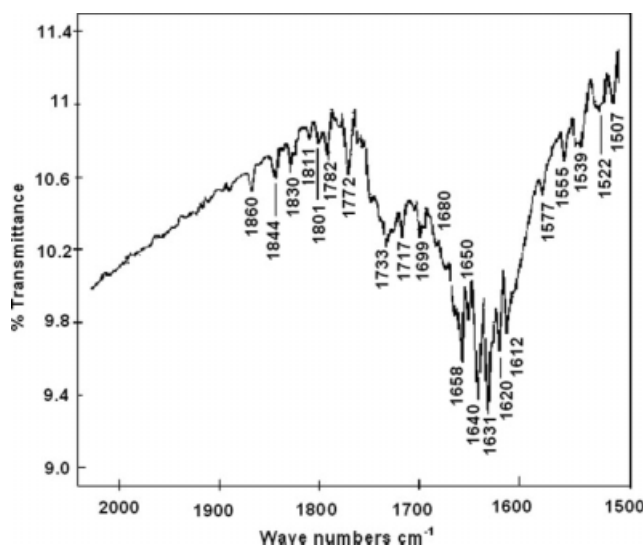


Figure 3 FTIR spectra of seaweed extract (2000–1600  $\text{cm}^{-1}$ ).

Secondary acyclic amides display a weak amide II band at  $1577 \text{ cm}^{-1}$  as a result of the presence of N–H bending vibration. The bands at  $1631$ ,  $1577$ , and  $1522 \text{ cm}^{-1}$  are consistent with the skeletal vibration of the aromatic system. The medium intensity of the band at  $1641 \text{ cm}^{-1}$  represents the C=C stretching. Primary amines exhibit medium-to-strong N–H in plane bending at  $1650 \text{ cm}^{-1}$ , which evolved to a slightly greater frequency in hydrogen-bonded molecules. The band at  $1658 \text{ cm}^{-1}$  was caused by C=C stretching with respect to the vinylidine group.<sup>24</sup>

The absorption bands at  $1680$  and  $1640 \text{ cm}^{-1}$  indicate C=O stretching (amide I band) and N–H in-plane bending (amide I band) vibrations, respectively, of the primary amide group. The absorption band at  $1699 \text{ cm}^{-1}$  was caused by the C=O absorption frequency. The effect of conjugation is at a maximum when the chromophores are coplanar. The steric effects, which disturb the coplanarity of the conjugated system, reduce the effect of conjugation. *cis*-nonplanar conjugation shift the C=O absorption at a greater frequency; thus, the coplanarity is lost and, consequently, the effect of conjugation is reduced.

The normal ketone will absorb at a frequency of  $1720 \text{ cm}^{-1}$ . The bands at  $1717$  and  $1733 \text{ cm}^{-1}$  are caused by carbonyl absorption. The normal ketone absorption is shifted as the result of  $\alpha$ -halo ketones. Because  $\alpha$ -halo ketones are a greater carbonyl absorption compound with the parent ketones and the shift increases with increasing dipole moment of C–X bond. This is due to the electrostatic interaction between two similarly oriented dipoles and is operative only when C–X and C=O bonds are approximately coplanar.

The halogen atom in equatorial orientation is near the carbonyl group, and the “field effect” causes an increase in the carbonyl stretching frequency. It shows the rigid molecule structure of  $\alpha$ -halo keto steroids.  $\alpha$ -halogen substitution increases in the C=O stretching frequency near  $1770 \text{ cm}^{-1}$ . The absorption bands near  $1782 \text{ cm}^{-1}$  show the presence of conjugated acyclic anhydride. The prominent absorptions at  $1830 \text{ cm}^{-1}$  represent asymmetric C=O stretching vibration of an acyclic anhydride group since the higher frequency C=O band is more intense.

The strong band at  $1860$  and  $1772 \text{ cm}^{-1}$  is the characteristic spectral feature of the C=O stretching absorption of an acid halide. Acid halide exhibit strong C=O stretching absorption in this region.

FTIR spectral data and spectrum show new signals, one at  $1733 \text{ cm}^{-1}$  (assigned to the C=O stretching vibration of a carboxyl acid group) and another, a small signal at  $817.8 \text{ cm}^{-1}$ , which was at lower wave number than the expected value for the S–O stretching vibration of primary sulphate group ( $820 \text{ cm}^{-1}$ ).<sup>22</sup> The absence of peak in the region of  $800$ – $1000 \text{ cm}^{-1}$  indicates that the extract not contains any 3,6-anhydrogalactosyl residues which will appear at  $930 \text{ cm}^{-1}$ .<sup>23</sup>

Figure 4 shows the spectrum of the  $4000$ – $2600 \text{ cm}^{-1}$  region. The bands at  $2923$  and  $2852 \text{ cm}^{-1}$  represent asymmetric and symmetric C–H stretching vibrations of alkyl groups in seaweed. The corresponding bending vibrations occur at  $1733 \text{ cm}^{-1}$ , respectively. The weak band at  $3453 \text{ cm}^{-1}$  occurs because of the stretching vibrations of free N–H. It

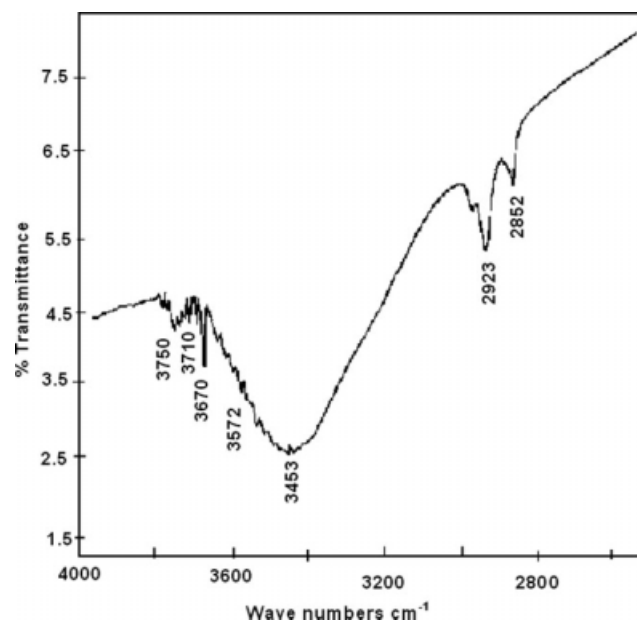
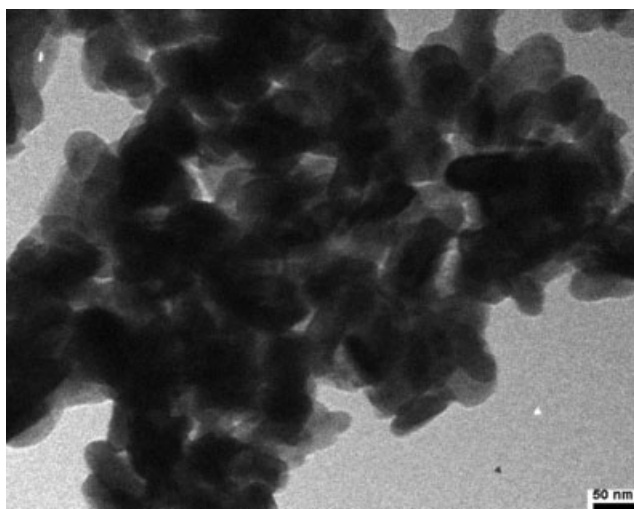


Figure 4 FTIR spectra of seaweed extract ( $4000$ – $2900 \text{ cm}^{-1}$ ).



**Figure 5** TEM image of seaweed extract at 50 nm.

indicates the *trans*-configuration of a secondary amide. The prominent O—H stretching bonded absorption was obtained in the range at  $3750\text{ cm}^{-1}$  and  $3710$  and  $3670\text{ cm}^{-1}$ .<sup>22,25</sup> The additional bands at  $3572$  and  $3453\text{ cm}^{-1}$  appear at lower frequency because of the intermolecular hydrogen bonding of the free hydroxyl group.

### TEM studies

A TEM image at greater magnification of the extracted seaweed powder is shown in Figure 5. It is clearly observed that the extracted granules of seaweed are in the nanometer scale range and possess different shapes. The variation of both shape and size among the granules may be due to the nature and the shape of various functional groups present in the extract.

### Antibacterial test

From the antibacterial activity test, the inhibition zone height of 3 mm is noted. This inhibition zone confirms the antibacterial activity of the acetone-extracted particles. The presence of groups such as amine, sulfate, bromine, and phenols<sup>12,26</sup> may be the reason for the antibacterial activity of the seaweed extract. While the amine absorbs the bacteria, it consequently stops the production of new bacteria and retards the cellular metabolism, thereby killing the bacteria. In conclusion, that the acetone extracts shows good antibacterial activity like other solvents.<sup>15,17,20,27</sup> When the finished fabric gets washed with water, the applied extract goes off and hence the amine group content diminished thereby the antibacterial strength is weakened.

### CONCLUSIONS

The analysis of the extract by UV–visible spectroscopy confirms the presence of carbonyl group with absorption band at 281 nm,  $\alpha$  and  $\beta$  unsaturated ketone in the 350–370 nm region, and the presence of nitroso group band at 662 nm. FTIR was used to confirm the presence of amide group with the appearance of peaks at  $644$  and  $531\text{ cm}^{-1}$ , which was caused by the O—C—N bending vibration. The presence of sulfate group is also confirmed by a strong absorbance at  $1273\text{ cm}^{-1}$  and is caused the S=O asymmetric stretching vibration of sulphate groups, whereas the band at  $583\text{ cm}^{-1}$  is caused by the O—S—O asymmetric deformation of sulphate group. A strong band observed at  $3670\text{ cm}^{-1}$  can be attributed to unbonded hydroxyl group of alcohols and phenols. TEM shows the presence of nanometric granules of seaweed with different shapes. Finally, the prepared acetone extracts possess a good antibacterial activity similar to diethyl ether solvent extract.

The authors are grateful to Dr. P. Manisankar, Professor and Head, Department of Industrial Chemistry for aiding fruitful suggestions and constant inspiration to finish the work.

### References

- Mucha, H.; Hofe, D.; Abfal, S.; Swerev, M. *Melliand Textilber* 2002, 82, 238.
- Lo, L. Y.; Li, Y.; Yeung, K. W.; Yuen, C. W. M. *Int J Nanotechnol* 2007, 4, 667.
- Kale, M. J.; Bhat, N. V.; Gore, A. V.; Walunj, V. *BTRA Scan* 2008, 38, 9.
- Vigneshwaran, N.; Kumar, S.; Kathe, A. A.; Varadarajan, P. V.; Prasad, V. *Nanotechnology* 2006, 17, 5087.
- Li, Q.; Chen, S.-L.; Jiang, W.-C. *J Appl Polym Sci* 2007, 103, 412.
- Yadavm, A.; Prasad, V.; Kathem, A. A.; Rajm, S.; Yadavm, D.; Sundaramoorthym, C.; Vigneshwaranm, N. *Bull Mater Sci* 2006, 29, 641.
- Parthiban, M.; Gunasekaran, S. *Melliand Int* 2007, 13, 362.
- Salleh, A.; Wakid, S. A. *Malaysian J Sci* 2008, 27, 19.
- Senthilkumar, R.; Vijayaraghavan, K.; Thilakavathi, M.; Iyer, P. V. R.; Velan, M. *Biochem Eng J* 2007, 33, 211.
- Sreenivasa Rao, P.; Parekh, K. S. *Bot March* 1981, 24, 577.
- Chandini, S. K.; Ganesan, P.; Bhaskar, N. *Food Chem* 2008, 107, 707.
- Devi, K. P.; Suganthi, N.; Kesika, P.; Pandian, S. K. *BMC Complementary Alternative Med* 2008, 8, 38.
- Sheu, J.-H.; Wang, G.-H.; Sung, P.-J.; Duh, C.-Y. *J Nat Prod* 1999, 62, 224.
- Tuney, I.; Cadirci, B. H.; Dilek, U. D.; Sukatar, A. *Fresenius Environ Bull* 2007, 16, 428.
- Kumar, K. A.; Rengasamy, R. *Botanica Marina* 2000, 43, 409.
- Lima-Filho, J. V. M.; Carvalho, A. F. F. U.; Freitas, S. M.; Melo, V. M. M. *Braz J Microbiol* 2002, 33, 311.
- Febles, C. I.; Arias, A.; Gil-Rodriguez, M. C.; Hardisson, A.; Sierra Lopez, A. *Anuario del Instituto de Estudios Canarios* 1995, 34, 181.
- Ganesan, M.; Thirupathi, S.; Sahu, N.; Rengarajan, N.; Veeragurunathan, V.; Jha, B. *Curr Sci* 2006, 91, 1256.

19. Kubanek, J.; Jensen, P. R.; Keifer, P. A.; Sullards, C.; Collins, M. D. O.; Finical, W. *Proc Natl Acad Sci USA* 2003, 100, 6916.
20. Selva Subha, A.; Vijay Anand, A.; Anita Hebsiba, G.; Thambidurai, S. *Colourage* 2007, 54, 80.
21. Conley, R. T. *Infrared Spectroscopy*; Allyn and Bacon: Boston, 1972.
22. Nakamoto, K. *Infrared and Raman Spectra of Inorganic and Coordination Compounds*, 4th ed.; Wiley-Interscience: New York, 1986.
23. Matsuhira, B.; Conte, A. F.; Damonte, E. B.; Kolender, A. A.; Matulewicz, M. C.; Mejias, E. G.; Pujolb, G. A.; Zúñigaa, E. A. *Carbohydr Res* 2005, 340, 2392.
24. Silverstein, R. M.; Bassler, G. C.; Morill, T. C. *Spectrometric Identification of Organic Compounds*; Wiley: New York, Chichester, 1991.
25. Stancioff, D. J.; Stanley, N. F. *Proc Int Seaweed Symp* 1969, 6, 595.
26. Murphy, V.; Hughes, H.; McLoughlin, P. *Water Res* 2007, 41, 731.
27. Sastry, V. M. V. S.; Rao, G. R. K. *Botanica Marina* 1994, 37, 357.